2.A.1: 2.D

Nuclear Physics **A166** (1971) 605—623; © *North-Holland Publishing Co., Amsterdam*

(p, xn) REACTIONS INDUCED IN ^{169}Tm, ^{181}Ta AND ^{209}Bi WITH 20 TO 45 MeV PROTONS

C. BIRATTARI, E. GADIOLI, A. M. GRASSI STRINI,
G. STRINI, G. TAGLIAFERRI and L. ZETTA

Istituto di Fisica dell'Università, Milano

and

Istituto Nazionale di Fisica Nucleare, Sezione di Milano

Received 16 November 1970
(Revised 18 January 1971)

Abstract: The excitation functions of the reactions ^{169}Tm, ^{181}Ta and ^{209}Bi (p, xn) for $x = 3, 4$ have been measured at proton energies from 20 to 45 MeV. The experimental curves are analysed in terms of a sum of statistical and pre-compound contributions, the last one evaluated according to the model proposed by Griffin and Blann. The cross section for pre-compound neutron and proton emission appears to constitute a relevant portion of the total reaction cross section σ_R in all the energy interval examined. Correspondingly, the fraction of σ_R accounted for by the compound nucleus formation cross section is found to be as low as some 30 % for $30 \lessapprox E_p \lessapprox 40$ MeV.

E | NUCLEAR REACTIONS ^{169}Tm, ^{181}Ta, ^{209}Bi(p, xn), $E_p = 20-45$ MeV; measured $\sigma(E)$ for production of ^{166,167}Yb, ^{178,179}W, ^{206,207}Po. Natural targets.

1. Introduction

The (i, xn) reactions offer a promising approach to the study of the interaction mechanisms of a beam of incident particles i with target nuclei. As is well known, the excitation functions of this type of reactions exhibit a bell-shaped pattern, with a rather broad top. The compound nucleus (CN) picture of the process predicts this behaviour but fails to account for the high-energy tail of the excitation functions. This tail is assumed to derive from a non-compound process, by means of which the incident particle can eject a neutron from the target nucleus before the CN is formed, that is before thermal equilibrium is reached between the nucleons. When such is the case, the resulting residual nuclei will have low excitation energies, and the neutrons emitted in the subsequent evaporation process will be fewer than expected if all the incident energy were to go in CN formation. The first problem in the interpretation of the experiments is then to determine the partial cross sections for the two interaction mechanisms.

At high energies, a model due to Serber describes the non-compound mechanism assuming free interactions between the incident projectile and the nucleons of the target, considered as a Fermi gas nucleus. The model, with various degrees of sophistication, has been utilized to describe the interaction of projectiles of energy higher than or equal to 80–100 MeV, and although affected by the critical dependence of the results on the parameters introduced, seems able to predict the main features of the experimental data [1]). The model, however, can hardly be extended to energies lower than those quoted above. In fact as the bombarding energy is lowered, the principal assumptions of the model are no longer fulfilled: (i) the wavelength of the projectile is greater than the mean distance between nucleons, (ii) the collision time is not much shorter than the collision time between nucleons inside the nucleus, and (iii) the residual interaction energy between nucleons is not negligible in comparison with the energy exchanged during nucleon-nucleon collisions. It is noteworthy that Verbinsky and Burrus have recently extended the model to energies as low as 15 MeV [ref. [2])], but the success reported by these authors might be attributed to an appropriate choice of the parameters used rather than to the adequacy of the model in the low-energy region.

Griffin [3]) and Blann [4]) have introduced a new model to describe the emission of nucleons from an intermediate system before thermal equilibrium. The mode of decay of this system is called pre-compound emission. The basic idea of the model is that the interaction of the projectile with the target gives rise first to a few-particle-hole configuration; the statistical equilibrium configuration corresponding to CN is approached through nucleon-nucleon interactions. In the first stages of the process the available excitation energy is shared between few degrees of freedom, and a relatively high possibility exists that a nucleon is emitted. Assuming two-nucleon interactions it is possible to calculate the spectral distribution for precompound nucleon emission. The model, although yet unrefined, has been applied with success in the study of particle spectra from (p, n) and (α, p) reactions and in the analysis of several (α, xn), (p, xn), (p, pxn) excitation functions [3, 4]).

To conclude the introductory remarks, it should be added that the CN contribution to the excitation functions can be calculated with the standard procedures of the equilibrium statistical model. The problems encountered are those of a correct choice of the parameter values, and of a sensible assessment of the effects of the approximations introduced.

1.1. PURPOSE OF THE PRESENT WORK

This paper reports the results of an experiment performed to measure the excitation functions for (p, 3n) and (p, 4n) reactions induced in ^{169}Tm, ^{181}Ta and ^{209}Bi with 20 to 45 MeV protons. The research was prompted by the lack of accurate data in an energy region where the presence of both direct effects and CN formation is expected to be comparable. Furthermore, a choice of target nuclei was made which spans the heavy nuclei region below the high fissility elements.

The aim of the analysis was to extract from the experimental results quantitative information concerning the relative importance of the pre-compound and CN mechanisms. To reach reliable conclusions, the values of the parameters introduced in the

CN calculation are chosen *a priori*, and no adjustment is allowed in order to fit the present data. The conclusions of the analysis will finally be compared with the results from (p, α) reactions on heavy nuclei studied in this laboratory [5]) and elsewhere [6]).

2. Experimental method and results

The excitation functions of the reactions ^{169}Tm(p, xn), ^{181}Ta(p, xn), and ^{209}Bi (p, xn), for $x = 3$ and 4, have been determined using the technique of radioactivity measurements. The irradiations were carried out in the external beam of the Milan AVF cyclotron [7]), with protons of 18 to 45 MeV. Although some of these excitations functions were measured in the past [8]), substantial improvement of the results can be obtained today, owing to the availability of better quality beams and high-resolution semiconductor detectors.

Two Ge(Li) spectrometers were used in the present work: one was a γ-ray detector with 2.2 keV resolution at 600 keV, the other an X-ray detector with 350 eV resolution at 20 keV. For the determination of the shape of the excitation function, a suitable γ-line free from interfering activities was chosen. The absolute value of the cross section was determined by the measurement of X-ray activity at an incident proton energy corresponding to the maximum of the excitation function. The high resolution of the X-ray spectrometer enabled us to discriminate against rays from adjacent elements produced in competing (p, xn) and (p, p($x-1$)n) reactions. No chemical separation of reaction products was needed.

2.1. TARGETS AND IRRADIATIONS

Thulium and tantalum targets were obtained from commercially available foils, 20 μm thick. Bismuth targets were prepared in this laboratory by evaporating granular Bi in 2 cm $\times$ 2 cm foils 30 mg/cm^2 thick. For the irradiation, the targets were placed inside a Faraday cup which secured complete beam charge collection. The Faraday cup was in the centre of a 65 cm scattering chamber. This arrangement also permitted an accurate energy monitoring of the beam.

Beam currents ranging from about 10 to 100 nA were used, so that in most cases only a few minutes of well-controlled irradiation were necessary to excite the required activities in the targets.

2.2. BEAM MONITORING

For an accurate determination of the shape of the excitation function in the neighbourhood of the reaction threshold, the energy spread of the beam should be the lowest possible. In the majority of the runs this spread was contained within 200 keV [ref. [7])]. The absolute energy of the beam was measured with the crossover technique [9]) below 30 MeV, and deduced from the radius of the last orbit inside the cyclotron above 30 MeV. In both cases the error in the determination is estimated to be less than ± 150 keV.

To check the reliability of the charge collection system, the cross section for the $^{12}C(p, pn)^{11}C$ reaction was measured at 42 MeV, and the result compared with that of Cumming [10]. The target activity was obtained by measuring the 511 keV annihilation radiation with a Ge(Li) detector calibrated with a standard ^{22}Na source. Agreement with the Cumming values was within 3 %. On account of this satisfactory result, the use of monitor targets was deemed unnecessary, and all the cross sections were derived from activity and charge collection measurements.

TABLE 1
Gamma lines used to obtain the excitation curves

Reactions	$T_{\frac{1}{2}}$	γ-line used
$^{169}Tm\ (p, 3n)^{167}Yb$	18 min	113.3 keV
$^{169}Tm\ (p, 4n)^{166}Yb$	58 h	X_K
$^{181}Ta\ (p, 3n)^{179}W$	38 min	30.7 keV
$^{181}Ta\ (p, 4n)^{178}W$	22 d	93.2 keV [a]) + X_K
$^{209}Bi\ (p, 3n)^{207}Po$	5.7 h	405.7 keV
$^{209}Bi\ (p, 4n)^{206}Po$	8.8 d	286.5 keV

a) From ^{178}Ta decay.

TABLE 2
Correction factors applied to the measured X-ray yields

Reactions	$\frac{X_K \text{ capture}}{X_K \text{ totals}}$	Ref.
$^{169}Tm\ (p, 3n)^{167}Yb$	0.50	[11]
$^{169}Tm\ (p, 4n)^{166}Yb$	0.73	[12]
$^{181}Ta\ (p, 3n)^{179}W$	0.99	[13]
$^{181}Ta\ (p, 4n)^{178}W$	1.00	[14]
	measured X_{Hf}	
$^{209}Bi\ (p, 3n)^{207}Po$	0.93	[15]
$^{209}Bi\ (p, 4n)^{206}Po$	0.70	[16]

2.3. CROSS-SECTION DETERMINATIONS

The γ-lines used to obtain the excitation curves are listed in table 1. For the reaction $^{169}Tm(p, 4n)^{166}Yb$ no suitable γ-peak is available, and the X_K radiation was used instead. Relative errors in these measurements resulting from statistics, target non-uniformities, calibrations, etc., are estimated to be of the order of 5 %. The K X-ray intensity determination from which the absolute cross sections are derived, must be corrected for the presence of X-rays due to K-conversion processes. The correction factors (X_K capture/X_K total) are reported in table 2; their values were estimated from the known conversion coefficients [11-16]. In the case of the $^{181}Ta(p, 4n)^{178}W$

reaction, the Hf K X-rays were measured in place of the Ta X-rays, owing to the large L/K capture ratio in ^{178}W. One further correction must be applied to take into account the self-absorption of the target for X- and low-energy γ-rays; it was determined directly using non-irradiated targets as absorbers.

A test of the results on the cross sections has been carried out with a sandwich arrangement. Two targets were mounted with an aluminium absorber in between, and exposed to the beam. The thickness of the absorber was the one needed to lower the beam energy from that corresponding to the flat maximum of the (p, 4n) curve to that of the (p, 3n) maximum. In this way the effects of the straggling in the absorber [less than 8 % FWHM of the energy absorbed [17]] are minimized. The test confirmed the results obtained.

The excitation functions measured in the present work are given in figs. 1–6. The error bars represent total errors in absolute values. Precise evaluation of these errors is made difficult by possible faults in some decay schemes reported in the literature. The consistency however of X_K- to γ-ray intensity ratios with values already published indicates that uncertainties of 10 % may be a fair assessment.

3. Analysis of the experimental data

As noted in the introduction, to interpret the shape of the excitation functions both statistical and non-statistical effects have to be taken into account. In the case of the present experiment, the contributions from the two types of effects add incoherently, since (i) the energy resolution of the proton beam was quite low, and (ii) transitions to many possible final states contribute to each reaction. Then, if σ_{CN} indicates the compound nucleus formation cross section, and σ_{DI}^{n} the cross section for precompound neutron emission, the following expression holds for the total (p, xn) cross section at a given incident energy E_i:

$$\sigma_{p,xn}(E_i) \approx \sigma_{CN}(E_i)P_{xn}(E)+\sigma_{DI}^{n}(E_i)\frac{\int_0^{U_{max}} P(E, U)P_{(x-1)n}(U)\mathrm{d}U}{\int_0^{U_{max}} P(E, U)\mathrm{d}U}, \tag{1}$$

where $P_{xn}(E)$ and $P_{(x-1)n}(U)$ are respectively the probabilities of emitting x and $(x-1)$ neutrons from the CN and the residual nucleus, after precompound neutron emission; E is the CN energy and $P(E, U)$ is the energy distribution of nuclei after precompound neutron emission.

3.1. CN CONTRIBUTION. GENERAL REMARKS

The analysis of the (p, xn) excitation functions in the framework of the statistical model leads to well-known formulae (see appendix 1) that require, except for x equal to 1 or 2, so many integrations as to make the numerical calculations impractical. Therefore, several approximations are usually introduced.

One of these consists in neglecting angular momentum effects. This approximation, however, leads to inconsistent results for (i, xn) reactions on nuclei in the same mass region when the incident particles are different. For low excitation energies, a high value of the angular momentum of the excited nuclei reduces neutron emission against charged particle or γ-ray emission.

A procedure that simplifies the calculation, and still allows one to take into account the main features connected with angular momentum effects, follows from the assumption that in the neutron decay of excited nuclei of spin J no levels are available to residual nuclei at energies lower than $E_{\mathrm{rot}} = J(J+1)\hbar^2/2\mathscr{I}$ (J is the average angular momentum of the CN created by the absorption of the projectile in the target). The reasonableness of the resulting approximation has been demonstrated by detailed numerical evaluations [18, 19]. The assumption itself is based on the fact that the neutron carries away energy but not angular momentum, whilst no levels of a given spin are present at energies lower than the "classical" rotational energy pertaining to the given angular momentum. Consequently, a nucleus having an excitation energy lower than or equal to the sum of the neutron binding energy, the pairing energy and the rotational energy of the residual nucleus, cannot emit further neutrons.

The introduction of the rotational energy increases the apparent threshold of the reaction and shifts the excitation functions toward higher energies. Other kinds of approximations which are acceptable in the heavy element region consist of assuming that the total width for particle emission from excited nuclei is equal to the neutron width, and that each emitted neutron carries away its average kinetic energy. As a consequence of the two last approximations, the calculation of the CN contribution to (p, xn) excitation functions is greatly simplified. How this is brought about is shown in appendix 1.

3.2. CHOICE OF PARAMETERS FOR THE CN CALCULATION

The actual calculation of neutron emission following the CN formation requires a choice of the best numerical values of a number of parameters. Some of these parameters (for instance the binding energies of the emitted neutrons and the pairing energies of the residual nuclei) strongly influence the outcome of the present calculation, others (like the level density parameters) have a far smaller effect. For other reactions, however, the relative importance of the various parameters can be different. In the case of (p, α) reactions in heavy nuclei, it is found [5]) that the results of the analysis are critically affected by the level density parameters. Therefore, to allow for consistent comparisons with other reaction data, it is desirable that all the parameters be carefully chosen.

The choice of parameters is specified below:

(i) The binding energies are the experimental ones taken from the paper of Liran and Zeldes [20]) or, when not available there, from Mattauch, Thiele and Wapstra [21]). If some experimental quantities were missing, values given by Wing and Varley [22]) are used; it would have been equivalent to use the very similar values of Myers and

Swiatecki [23]). Notice also that possible errors in the theoretically estimated binding energies would affect only the ^{181}Ta(p, xn) excitation functions.

(ii) For the pairing energies, average values were calculated from the figures given [ref. [24])] by Cameron in 1958 and 1965 and by Nemirovski and Adamchuck in 1962. These average values are expressed by the laws $\Delta_N = (1.374-0.00516N)$ MeV and $\Delta_Z = (1.654-0.00958Z)$ MeV.

(iii) In the expression of rotational energy, the rigid body moment of inertia is assumed with a radius $R = 1.27\ A^{\frac{1}{3}}$ fm.

(iv) The neutron inverse cross section is again a parameter of importance in the calculation [25]). The values assumed here are those of Lindner [26]), who used the non-local potential of Perey and Buck [27]).

(v) The choice of appropriate level density formulae and parameters requires a few comments owing to the fact that it would be inaccurate to utilize the Lang and Le Couteur [28]) expression with parameters inferred from slow neutron resonance spacings [29]) in the case of most of the nuclei and excitation energies of interest here.

Indeed it was shown in a recent paper from this laboratory [30]) that for near doubly magic nuclei a more complex expression is needed. This was deduced with the help of a simple model describing a magic shell nucleus as a two-fermion gas with an energy gap at the Fermi energy. The gap was taken equal to 1.43 MeV. The level density parameter a was still given by the empirical relation

$$a = (0.210N+0.025)\mathrm{MeV}^{-1}, \tag{2}$$

which reproduces the average trend of a-values outside the region affected by shell effects. This treatment applies to the case of ^{209}Bi(p, xn) reactions, with just the above parameters.

The nuclei involved in the reactions induced on Tm and Ta do not exhibit shell effects at slow neutron resonance energies. At excitation energies E higher than a minimum $E_{\min}$ characteristic of each nucleus, however, the gap model of ref. [30]) predicts the occurrence of shell effects. The determinations of $E_{\min}$ are reported in appendix 2; the results are as follows. For Tm and neighbour nuclei the average excitation energy $\langle E \rangle \lessapprox E_{\min}$; then no serious error is introduced by the use of the Lang and Le Couteur formula, with a given by eq. (2). For Ta and neighbouring nuclei, $\langle E \rangle > E_{\min}$; in first approximation, the Lang and Le Couteur expression can still be used, but with an effective a lower than indicated by (2); the value $a \approx 18$ MeV^{-1} is suggested.

The foregoing discussion on level densities in heavy nuclei applies also to the evaluation of charged particle emission rates, and therefore their consideration offers a means of testing the usefulness of the above procedure. In particular, results on (p, α) reactions, to be quoted in sect. 4, appear to support the present choices.

3.3. PRECOMPOUND CONTRIBUTION

The precompound contribution is evaluated according to the Griffin-Blann model. The decay rate for the emission of one nucleon from a nucleus in an n exciton state

($n = p+h$, the number of particles plus holes) is given by the expression

$$P_n(\varepsilon)\mathrm{d}\varepsilon = \frac{(2s+1)\mu\varepsilon\sigma_c(\varepsilon)}{\pi^2\hbar^3} \frac{\rho_{n-1}(U)}{\rho_n(E)} \mathrm{d}\varepsilon, \tag{3}$$

where s is the emitted particle spin, and $\rho_{n-1}(U)$ and $\rho_n(E)$ are the level densities for $n-1$ and n exciton states, E is the excitation energy of the intermediate system (projectile plus target), and U is the excitation energy of the residual nucleus. For the ^{181}Ta(p, xn) and ^{169}Tm(p, xn) reactions, E and U are given by the usual expressions

$$E = E_{\mathrm{inc}}+B_{\mathrm{inc}}-\Delta,$$

$$U = E_{\mathrm{inc}}+B_{\mathrm{inc}}-B_{\mathrm{out}}-\Delta_{\mathrm{R}}-\varepsilon,$$

where E_{inc} is the incident energy, B_{inc} and B_{out} the binding energies of the incident and outgoing particles, Δ and Δ_{R} the pairing energies of the intermediate system and of the residual nucleus, ε the emitted nucleon energy.

In the case of the ^{209}Bi(p, xn) reactions, according to the gap model of ref. [30]) the excitation energies have the above values if $p \approx \frac{1}{2}n < k$ (k being the number of particles above the gap). If $\frac{1}{2}n > k$, values reduced by the quantity $\Delta^* = (\frac{1}{2}n-k)(D-\bar{d})$ are assumed, where D is the energy gap and $\bar{d}$ the average nucleon spacing at the Fermi energy.

In the Griffin model the initial configuration of the intermediate system corresponds to an n' exciton state. This state can either decay by particle emission or proceed through nucleon-nucleon interactions towards an n'' exciton state. This state can in turn decay by particle emission or give rise to a new, more complicated configuration. Assuming two-body interactions, Δn can be either 0 or ± 2. On physical grounds, it is further assumed that Δn is equal to 2 if $n \ll \bar{n}$, where $\bar{n}$ is the average number of excitons at thermal equilibrium. This approximation is acceptable since the density of states corresponding to n excitons greatly increases with n until n approaches $\bar{n}$.

By introducing the expression for the level density of the n exciton states, assuming constant lifetimes for all these states and summing over all possible states, the expression for the energy distribution of residual nuclei in precompound nucleon emission is reached:

$$P(\varepsilon)\mathrm{d}\varepsilon \propto \frac{\varepsilon\sigma_c(\varepsilon)}{gE} \left[\sum_{\substack{n=n' \\ \Delta n=+2}}^{\bar{n}} \left(\frac{U}{E}\right)^{n-2} p(n-1) \right] \mathrm{d}\varepsilon. \tag{4}$$

The quantity g is given by $g = 6a/\pi^2$. All the parameters needed are chosen as in subsect. 3.2; n' has been taken equal to 3 as suggested by Blann.

The summation in eq. (4) converges rapidly when $U \ll E$; when U is not much lower than E, many terms are of importance and some doubt concerning the assumptions introduced could be raised. It must also be stressed that in deriving formula (4) the depletion of bound states due to particle emission was neglected.

Thus, for the time being, judgement on the consistency of the Griffin-Blann model must be reserved. Its ability, however, to account for the experimental results in the study of several (i, xn) and (i, pxn) excitation functions has been already indicated [4].

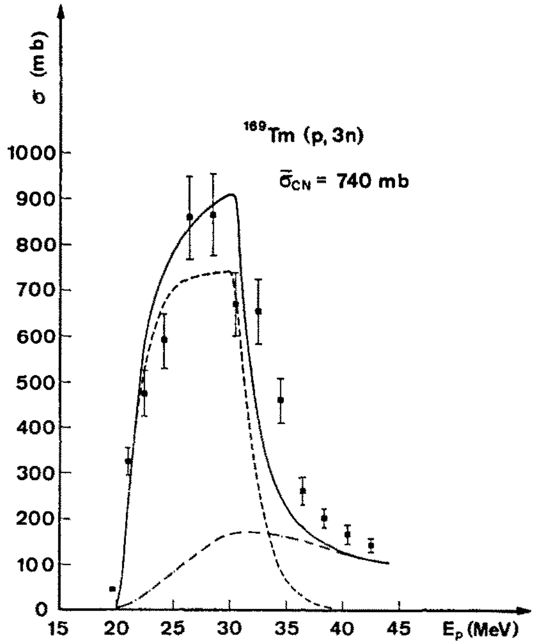

Fig. 1. Excitation function of the reaction ^{169}Tm(p, 3n). In all figs. 1 –6 the theoretical prediction, calculated according to (1), is shown as a solid line; the dashed and the dot-and-dashed lines give the contributions of the first and second term on the right-hand side of eq. (1). The CN contribution has been calculated assuming an average CN formation cross section equal to 740 mb.

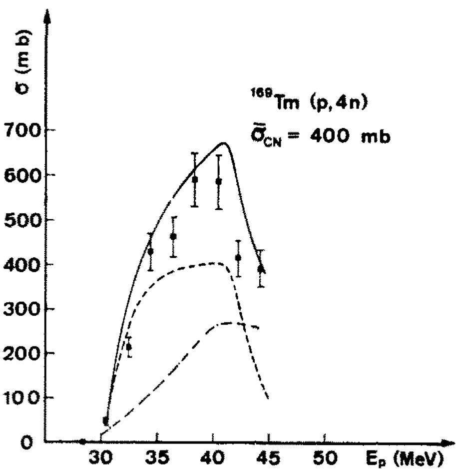

Fig. 2. Excitation function of the reaction ^{169}Tm((p, 4n). The CN contribution has been calculated assuming an average CN formation cross section equal to 400 mb.

and is confirmed here (cf. sect. 4). Whether this success is helped by accidental factors, like a partial compensation of different approximations, remains to be seen.

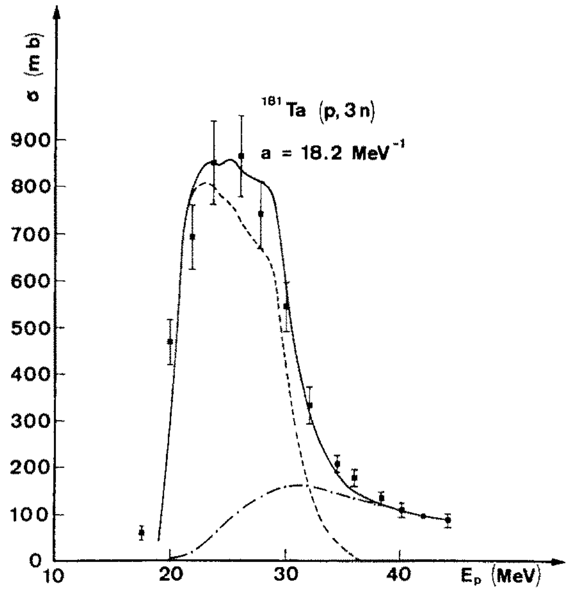

Fig. 3a. Excitation function of the reaction ^{181}Ta(p, 3n). The CN contribution has been calculated assuming a σ_{CN} variable with energy, as shown in fig. 11. The level density parameter is taken equal to 18.2 MeV^{-1}.

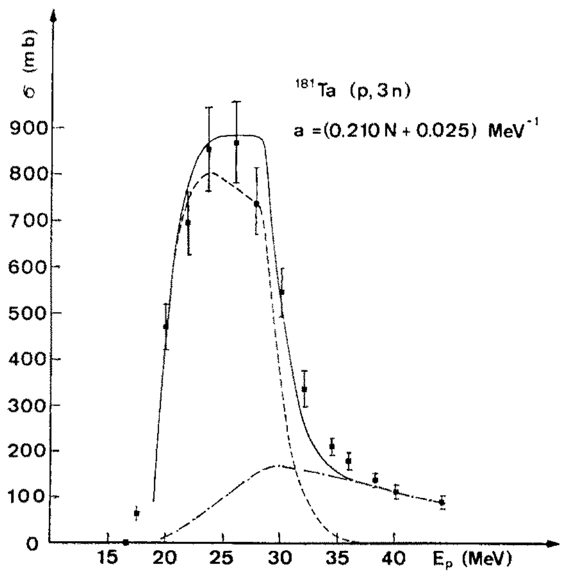

Fig. 3b. The same as fig. 3a, but with the level density parameter given by $(0.210N+0.025)$ MeV^{-1}.

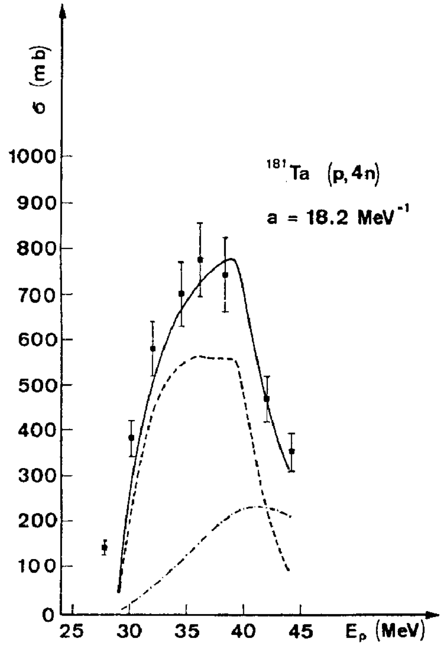

Fig. 4a. Excitation function of the reaction ^{181}Ta (p, 4n). The theoretical curves are calculated as in fig. 3a.

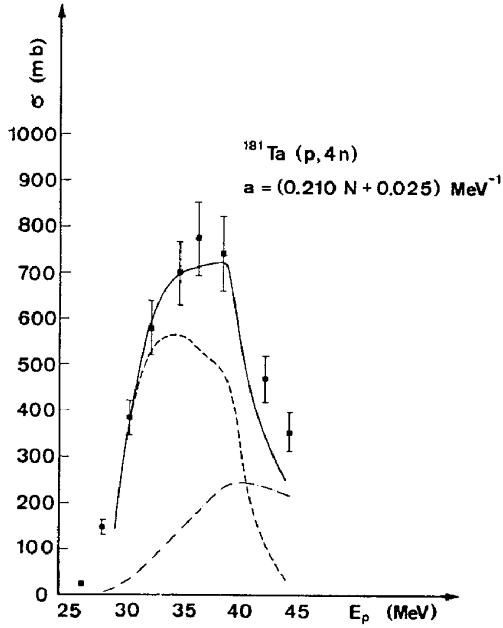

Fig. 4b. Excitation function of the reaction ^{181}Ta (p, 4n). The theoretical curves are calculated as in fig. 3b.

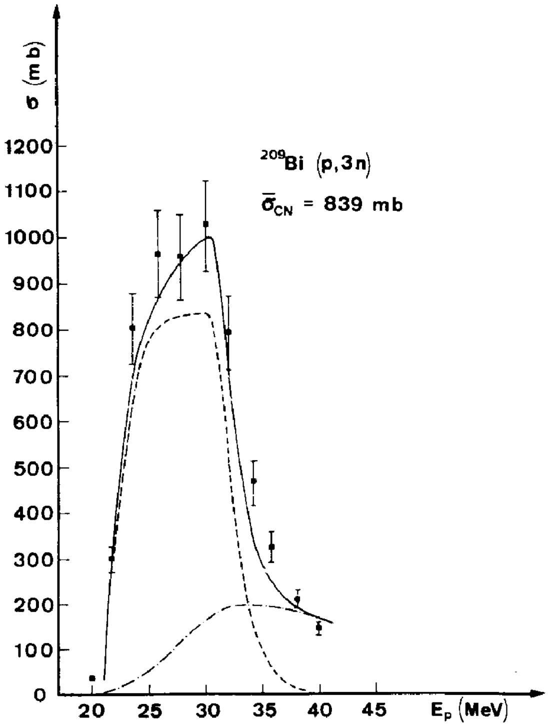

Fig. 5. Excitation function of the reaction ^{209}Bi(p, 3n). The CN contribution has been calculated assuming an average CN formation cross section equal to 839 mb.

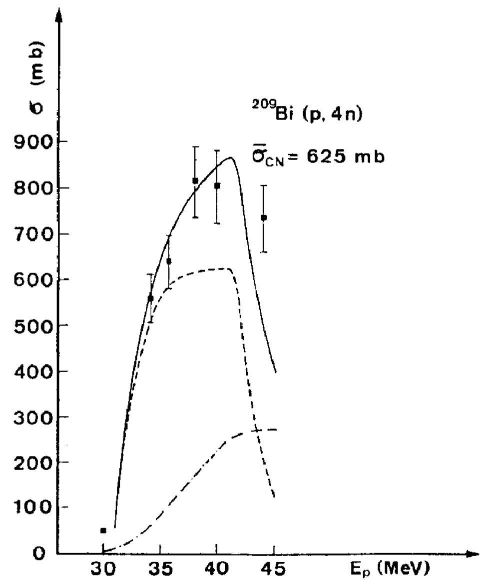

Fig. 6. Excitation function of the reaction ^{209}Bi(p, 4n). The CN contribution has been calculated assuming an average CN formation cross section equal to 625 mb.

4. Results of the analysis and discussion

The comparison of the excitation functions with the results of the analysis outlined in the previous section can be started by noticing that the tail of the experimental curves gives directly the percentage of non-compound effects, because at high energies the CN contribution is negligible. In all the reactions considered, the fit to the tail gives for σ_{DI}^{n} a value around 500 mb at $E_p \approx 40$ MeV. At $E_p \approx 18$ MeV, Verbinski

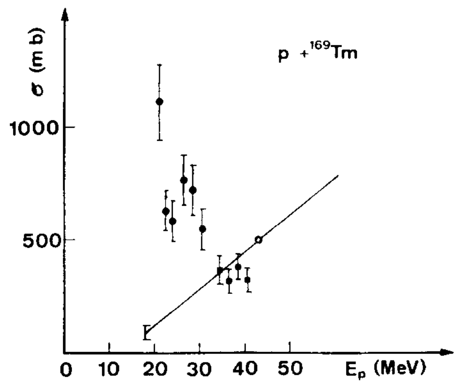

Fig. 7. Compound nucleus formation cross sections for protons on ^{169}Tm, obtained from the reactions ^{169}Tm(p, 3n) (black circles) and ^{169}Tm (p, 4n) (black squares). The assumed linear variation for the cross section corresponding to precompound neutron emission is also shown.

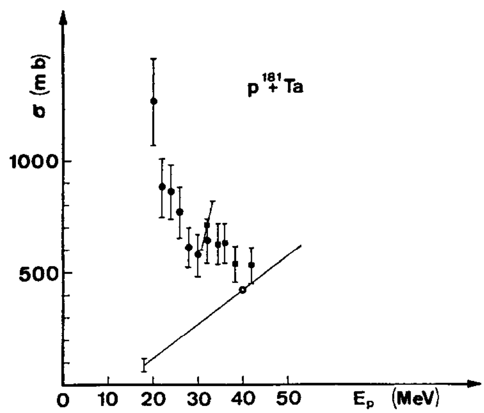

Fig. 8. The same as fig. 7 for protons on ^{181}Ta.

and Burrus [2]) reported, from the analysis of (p, n) spectra in nuclei of the same mass region, a σ_{DI}^{n} equal to about $0.1\sigma_{CN}$. This estimate suggests for σ_{DI}^{n} at $E_p \approx 18$ MeV a value comprised between 60 and 120 mb, assuming for σ_{CN} the limits of 600 and 1200 mb obtained by the extrapolation to low energies of the values at $30 < E_p < 40$ MeV, and by the optical-model evaluation of the total reaction cross section σ_R at 18 MeV. The energy dependence of σ_{DI}^{n} between 18 and 40 MeV is not known; the precompound theory is not yet able to answer this question. It is believed, however, that σ_{DI}^{n} should vary quite smoothly with energy, so that the arbitrary assumption of a linear variation in the above interval may not be too unreasonable. Both this hypothesis, and the great uncertainty of the σ_{DI}^{n} deduced for the lowest energy, are not expected to introduce serious errors in the present analysis, although the numerical results may be somewhat influenced.

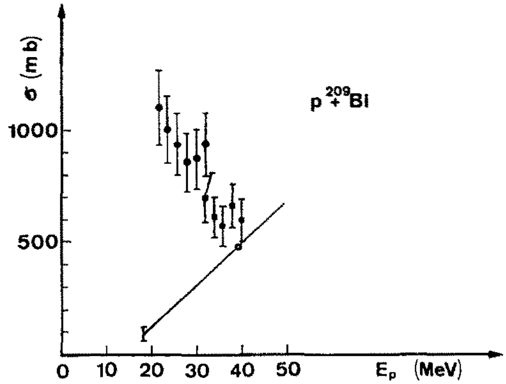

Fig. 9. The same as fig. 7 for protons on ^{209}Bi.

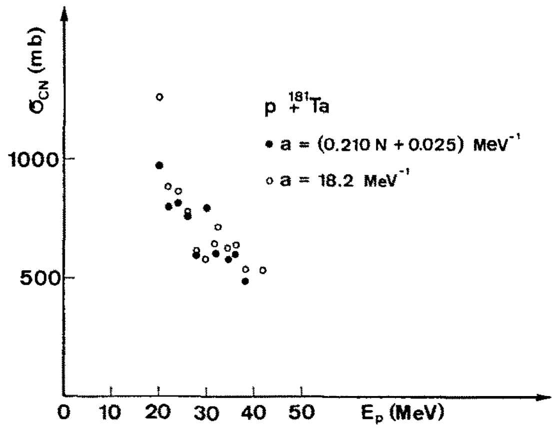

Fig. 10. Compound nucleus formation cross section for protons on ^{181}Ta; the effect of changing, as indicated, the value of the level density parameter is shown.

The precompound contribution is then calculated by using the σ_{DI}^{n} values, the energy distribution of residual nuclei after precompound emission, and the statistical model probability for $(x-1)$ neutron emission. This procedure stands on the hypothesis that a residual nucleus, after precompound neutron emission, can only proceed towards equilibrium with a subsequent statistical decay. The hypothesis that further precompound emission should be unlikely is obviously tentative; it is consistent, however, with the assumed energy distribution of residual nuclei, as expressed by eq. (4).

To complete the calculation, the CN contribution must be added. The final results are shown in figs. 1–6, where the fits to the experimental curves are reported. It is seen that in spite of the approximations introduced, the agreement reached is quite satisfactory. It should be emphasized that all the parameters entering the calculation have been fixed *a priori*, and are obtained by independent analyses of existing experimental data. The only quantities fixed by the fit to the present data are the relative percentages of precompound and CN effects.

In figs. 7–9 the CN formation cross sections, obtained from the experimental points in the peak region of the excitation functions, and the assumed linear variation of σ_{DI}^{n} with E_p are reported. The statement of subsect. 3.2 to the effect that the choice of the level density parameter a is not critical in the present analysis, is illustrated for the

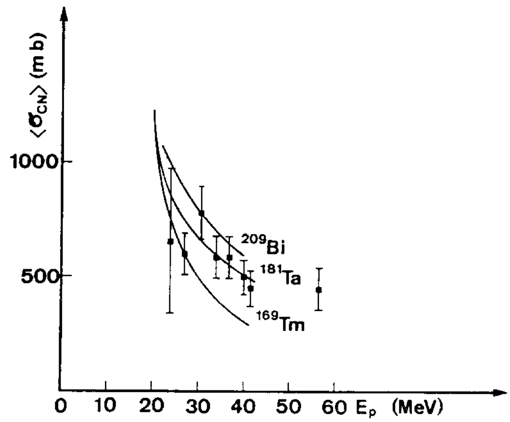

Fig. 11. Comparison between compound nucleus formation cross sections for protons on heavy nuclei, deduced from the (p, xn) reactions (solid lines) and from the ^{197}Au (p, α) reaction (black squares). The experimental data on which the (p, α) results are based are from ref. [5]) up to 42 MeV, and from ref. [6]) at 56 MeV.

reactions induced on ^{181}Ta by the comparison of figs. 3a and 4a with 3b and 4b, and in fig. 10 specifically for σ_{CN}. This fact, together with the adequate agreement between the σ_{CN} values for the reactions in the three elements studied, lends support to the rather unexpected results of the evaluation of σ_{CN}, which for $30 < E_p < 40$ MeV amounts to no more than about 30 % of the total reaction cross section.

The above conclusion can be compared with results now available for (p, α) reactions in heavy nuclei. Since α-particle emission from excited heavy nuclei is a quite improbable phenomenon, its occurrence is strongly dependent on the level densities of the nuclei implied in the statistical decay. Therefore, the analysis of the statistical contribution to the cross section for such reactions complements very aptly the one performed on (p, xn) data. In fig. 11, the agreement between the CN formation cross sections obtained in this work and in the analysis of the ^{197}Au(p, α) reaction [5]) is shown to be rather good. The parameters used to calculate the level densities of the nuclei involved in this reaction, have been estimated following the method outlined in appendix 2. Very reasonable accord is found also with the results inferred from the data of Muto *et al.* [6]); as a case of special interest here it may be mentioned that the ^{181}Ta(p, α) reaction, when analysed by assuming the effective a-value of $\approx$ 18 MeV^{-1}, yields results consistent with those from the ^{181}Ta(p, xn) reactions.

5. Conclusion

The study of (p, 3n) and (p, 4n) excitation functions for nuclei in the heavy mass region at E_p from 20 to 45 MeV suggests a very important contribution of precompound effects to the total reaction cross section. This conclusion confirms the one recently reached by Blann and Lanzafame, and extends its validity to reactions induced by protons in heavy elements.

The compound nucleus formation cross section is found to vary between about 1200 mb at E_p = 20 MeV and $\approx$ 500 mb at E_p = 40 MeV. Such low values were unexpected, and are at variance with those inferred by extrapolating from higher energies the results of Monte Carlo calculations of the non-compound effect [1]). The present values, however, appear to be quite consistent with the ones deduced from (p, α) reactions in nuclei of the same mass region. The results obtained suggest a great value for the sum of the cross sections corresponding to precompound emission of particles different from neutrons, and possibly to fission.

Taking into account that both experimental data [31]) and reasonable physical assumptions favour the case of precompound proton emission, a further progress towards the understanding of the reaction mechanism at these intermediate energies, in heavy nuclei, might come from a systematic study of (p, pxn) excitation functions.

The authors wish to acknowledge their indebtness to Dr. Marcel Barbier for discussions in the early stage of this work, to Dr. Michelangelo Fazio for preparing the Bi targets, and to Prof. Giancarlo Bertolini for advice and for the loan of some valuable equipment.

Appendix 1

This appendix reports the procedure used to calculate the (p, xn) cross sections according to the statistical model, and points out the approximations adopted.

The expression given by the said model for the cross section of a (p, 3n) reaction is the following:

$$\sigma(\text{p}, 3\text{n}) = \sigma_{\text{CN}}(\text{p}) \int_0^{E_n} G_1(\varepsilon_1) \left\{ \int_0^{E_n-\varepsilon_1} G_2(\varepsilon_2) \left[\int_{E_{3m}}^{E_n-\varepsilon_1-\varepsilon_2} G_3(\varepsilon_3)\mathrm{d}\varepsilon_3 \right] \mathrm{d}\varepsilon_2 \right\} \mathrm{d}\varepsilon_1, \qquad \text{(A.1)}$$

where $\sigma_{\text{CN}}(\text{p})$ is the CN formation cross section, and $G_1(\varepsilon_1)$, $G_2(\varepsilon_2)$, $G_3(\varepsilon_3)$ are the branching ratios for emission of the first, second and third neutron.

For physical reasons ε_3 cannot assume negative values. As a consequence the lower limit of integration of the innermost integral, E_{3m}, is equal either to $E'_n - \varepsilon_1 - \varepsilon_2$ when this quantity is positive, or to 0 when it is negative. The values of E_n and E'_n are obtained by imposing that

$$\varepsilon_1 + \varepsilon_2 + \varepsilon_3 + B_{1n} + B_{2n} + B_{3n} + \Delta_{3n} + E_{\mathrm{rot}\,3n} \leqq E_{\mathrm{CN}}, \tag{A.2}$$

i.e. emission of three neutrons is energetically possible, and

$$E_{\mathrm{CN}} - B_{1n} - B_{2n} - B_{3n} - \varepsilon_1 - \varepsilon_2 - \varepsilon_3 \leqq B_{4n} + \Delta_{4n} + E_{\mathrm{rot}\,4n}, \tag{A.3}$$

i.e. no energy is available for emission of a fourth neutron.

Relations (A. 2) and (A. 3) lead to

$$\begin{aligned}
&\varepsilon_1 \geqq 0, \\
&\varepsilon_1 \leqq E_{\mathrm{CN}} - B_{1n} - B_{2n} - B_{3n} - \Delta_{3n} - E_{\mathrm{rot}\,3n} = E_n, \\
&\varepsilon_2 \geqq 0, \\
&\varepsilon_2 \leqq E_n - \varepsilon_1, \\
&\varepsilon_3 \geqq E_{\mathrm{CN}} - B_{1n} - B_{2n} - B_{3n} - B_{4n} - \Delta_{4n} - E_{\mathrm{rot}\,4n} - \varepsilon_1 - \varepsilon_2 = E'_n - \varepsilon_1 - \varepsilon_2, \\
&\varepsilon_3 \leqq E_n - \varepsilon_1 - \varepsilon_2.
\end{aligned} \tag{A.4}$$

Each branching ratio is given as usual by:

$$G(\varepsilon) = \frac{g_n \mu_n \sigma_c(\varepsilon_n)\varepsilon_n \rho(E_c - S_n - \varepsilon_n, 0)}{\sum_j g_j \mu_j \int_0^{E_c - S_j} \sigma_c(\varepsilon_j)\varepsilon_j \rho(E_c - S_j - \varepsilon_j, 0)\mathrm{d}\varepsilon_j}, \tag{A.5}$$

where S_j is the sum of the binding and pairing energies for the emission of the given particle, and E_c is the energy available to the appropriate step of the decay chain.

The level densities are expressed either by the Lang and Le Couteur formula:

$$\rho(v, 0) = \frac{\hbar^3}{24\sqrt{8}} a^{\frac{1}{2}} \mathscr{J}^{-\frac{3}{2}} \frac{\exp[2\sqrt{av}]}{(v+t)^2}, \tag{A.6}$$

or, when shell effects are to be taken into account, by the gap model formula of ref. [30])

$$\rho^*(v, 0) = \rho(v', 0) \left\{ 1 - \frac{\frac{1}{3}g(D-\bar{d})}{\left[\left(\frac{1}{3\ln 2} - \frac{1}{3}g(D-\bar{d}) \right)^2 + \frac{2}{27(\ln 2)^2} \pi^2 g(v + k(D-\bar{d})) \right]^{\frac{1}{2}}} \right\}. \tag{A.7}$$

The assumptions that only neutron emission is possible (which is justified in the case of heavy nuclei were charged particle emission is negligible), and that each neutron carries away its average kinetic energy, offers a means to bypass the multiple integration in (A.1). What remains to be done instead is simply the evaluation of the energy spectrum of the first emitted neutron. The graph of fig. 12, together with its caption, illustrates the point.

Energy values E_1, E_2, etc., established as indicated, are used to break up the total area A under the energy distribution curve into partial areas A_1, A_2, etc. Then it is seen that if the emitted neutron energy falls e.g. into A_3, the residual nucleus can emit a second neutron with energy $\bar{E}_2$. The energy is further reduced by the quantity $B_{2n}+\Delta_{2n}-\Delta_{1n}$. The residual nucleus can emit a third neutron and the energy is still further reduced by the quantity $B_{3n}+\Delta_{3n}-\Delta_{2n}+\bar{E}_3$. The residual energy is now lower than $B_{4n}+\Delta_{4n}-\Delta_{3n}+E_{rot4n}$ and no more neutrons can be emitted. The probability for the emission of three neutrons is then given by the ratio $A_3/\sum_i A_i$ and the expression for the cross section of a (p, 3n) reaction reduces to

$$\sigma(\mathrm{p}, 3\mathrm{n}) \approx \sigma_{\mathrm{CN}}(\mathrm{p}) \frac{A_3}{\sum_i A_i}. \tag{A.8}$$

The extension to the case of (p, 4n) reactions is trivial.

Attention must be paid to evaluate correctly the average kinetic energies. These must be calculated at the excitation energy available for the step of the decay process from which the particle under consideration is emitted. We cannot expect that this

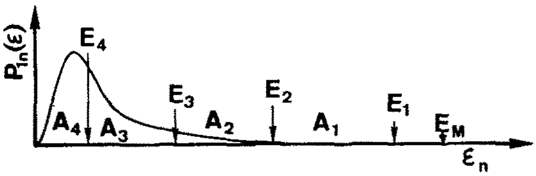

Fig. 12. Schematic plot of the energy spectrum of the first emitted neutron in a (p, xn) process. $E_M = E_{CN}-B_{1n}-\Delta_{1n}$; $E_1 = E_{CN}-B_{1n}-\Delta_{1n}-E_{rot\,1n}$; $E_2 = E_{CN}-B_{1n}-B_{2n}-\Delta_{2n}-E_{rot\,2n}$; $E_3 = E_{CN}-B_{1n}-B_{2n}-B_{3n}-\Delta_{3n}-\bar{E}_2-E_{rot\,3n}$; $E_4 = E_{CN}-B_{1n}-B_{2n}-B_{3n}-B_{4n}-\Delta_{4n}-\bar{E}_2-\bar{E}_3-E_{rot4n}$.

kind of calculation can give accurate results near threshold. The comparison with experimental data, however, shows that the calculated excitation functions agree with the experimental ones, if the binding energies are known, starting from values as low as one tenth of the maximum. This accuracy is sufficient for the analysis reported in this work.

Appendix 2

In this appendix the determination of the level density parameter a for nuclei involved in the reactions in Tm and Ta is discussed.

In the gap model of ref. [30]), shell effects on level density for magic nucleon numbers are attributed to a gap D at the Fermi energy.

Consider now nuclei, still in the heavy element region, with neutron and proton numbers less than respectively 126 and 82. It is known that the average occupation number of nucleon states around the Fermi energy, at an excitation energy E, is given by

$$n_s = \frac{1}{1+\exp\left(\frac{\varepsilon_s-\varepsilon_0}{t(E)}\right)}, \tag{A.9}$$

where ε_0 is the Fermi energy and $t(E)$ the thermodynamic temperature. To simplify the discussion, (A.9) is approximated by two squared distributions defining the same number of excited particles and holes. The width of these distributions around the Fermi energy is $E/(gt\ln 2)$. Shell effects do not influence the level density if

$$\Delta E^{\dagger} = \tfrac{1}{2}[(126-N)d_{\mathrm{n}}+(82-Z)d_{\mathrm{p}}] > E/(gt \ln 2), \tag{A.10}$$

i.e. if the mean distance between the last occupied nucleon state and the gap is greater than the maximum energy of excited nucleons.

If inequality (A. 10) is not satisfied, a decrease in level density should be expected. Formulae derived in ref. [30]) for near doubly magic nuclei can again give a first approximation of the correct level density expression if the excited nucleons occupy on the average levels above the gap; that is, if

$$\frac{E}{2gt \ln 2} > \Delta E^{\dagger}+D. \tag{A.11}$$

Inequalities (A.10) and (A.11) define two energies E_1 and E_2.

Below E_1 no shell effects influence the level density, the usual Lang and Le Couteur formula applies and a is given by the law $a \approx (0.210N+0.025)\ \mathrm{MeV}^{-1}$; above E_2 expression (A.7) could be used, or, alternatively, in the Lang and Le Couteur formula a reduced effective value for a should be introduced by imposing that the two level densities expressions give the same absolute value. Between E_1 and E_2 the level density function is unknown, but it must join smoothly to the values assumed at E_1 and E_2. This fact implies that if Lang and Le Couteur expression is used as an interpolation formula for $E_1 < E < E_2$, and $E_2 \gg E_1$, the reduced a-value for $E \approx E_2$ can be taken as a lower estimate of a in the interval from E_1 to E_2.

When the nuclei studied in this work are considered, one finds: for ^{169}Tm and its neighbours, $E_1 \approx$ 33–41 MeV, $E_2 >$ 240 MeV; for ^{181}Ta and its neighbours, $E_1 \approx$ 16–20 MeV, $E_2 \approx$ 145–170 MeV. Therefore, since the incident energy around the maximum of the excitation function is definitely higher than E_1 in the second case, while it is of the order of E_1 in the first, a reduced a-value is employed only in the analysis of the reactions induced in ^{181}Ta.

One final remark may be added concerning deformation effects. These, as shown by Strutinsky [32–33]), could reduce the a-values at low excitation energies. For the cases of interest here, however, it has been calculated that the nucleon state density at the Fermi energy is not appreciably modified owing to nuclear deformations.

References

1) N. Metropolis, R. Bivins, M. Storm, A. Turkevich, J. M. Miller and G. Friedlander, Phys. Rev. **110** (1958) 185;
H. W. Bertini, Phys. Rev. **131** (1963) 1801;
J. P. Cohen, Nucl. Phys. **84** (1966) 316;
K. Chen, Z. Fraenkel, G. Friedlander, J. R. Grover, J. M. Miller and Y. Shimamoto, Phys. Rev. **166** (1968) 949
2) V. V. Verbinsky and W. R. Burrus, Phys. Rev. **177** (1969) 1671
3) J. J. Griffin, Phys. Rev. Lett. **17** (1966) 488; Phys. Lett. **24B** (1967) 5
4) M. Blann, Phys. Rev. Lett. **21** (1968) 1357;
M. Blann and F. M. Lanzafame, Nucl. Phys. **A142** (1970) 559
5) E. Gadioli, I. Iori, N. Molho and L. Zetta, to be published
6) J. Muto, H. Itoh, K. Okano, N. Shiomi, K. Fukuda, Y. Omori and M. Kihara, Nucl. Phys. **47** (1963) 19
7) E. Acerbi, C. Birattari, M. Castiglioni, G. Dutto, G. Fait, G. Strini and C. Succi, Proc. Int. Conf. on cyclotrons, Oxford (1969)
8) C. L. Rao and L. Yaffe, Can. J. Chem. **41** (1963) 2516;
R. E. Bell and H. M. Skarsgard, Can. J. Phys. **34** (1956) 745
9) R. Smythe, Rev. Sci. Instr. **35** (1964) 1197
10) J. B. Cumming, Nucl. Phys. **49** (1963) 417
11) K. Y. Gromov, A. S. Danagulyan, A. T. Strigachev and V. S. Shpinel, Sov. J. Nucl. Phys. **1** (1965) 276;
R. G. Wilson and M. L. Pool, Phys. Rev. **120** (1960) 1296
12) A. Jasinski, J. Kownacki, H. Lancman, J. Ludziejewski, S. Chojnacki and I. Yutlandov, Nucl. Phys. **41** (1963) 303
13) C. Birattari, G. Strini, G. Tagliaferri and G. Bertolini, Nuovo Cim. Lett. **2** (1969) 473;
J. Konijn, B. J. Meijer, B. Klank and R. A. Ristinen, Nucl. Phys. **A137** (1969) 593
14) G. Wilkinson, Phys. Rev. **80** (1950) 495;
C. J. Gallaghen, Jr., H. L. Nielsen and O. B. Nielsen, Phys. Rev. **122** (1961) 1590;
J. H. Hamilton, A. V. Ramayya, B. Van Nooijen, R. G. Albridge, E. F. Zganjar, S. C. Pancholi, J. M. Hollander, V. S. Shirley and C. M. Lederer, Nuclear Data **A1** (1966) 521
15) E. Arbman, J. Burde and T. R. Gerholm, Ark. Fys. **13** (1958) 501
16) E. Arbman, Nucl. Phys. **3** (1957) 625;
C. M. Lederer, J. M. Hollander and I. Perlman, Table of isotopes (Wiley, New York, 1968)
17) H. D. Maccabee, Proc. Int. Conf. on cyclotrons, Oxford (1969);
J. J. Kolata and T. M. Amos, Phys. Rev. **176** (1968) 484;
C. Tschalär, Nucl. Instr. **61** (1968) 141; **64** (1968) 237
18) J. R. Grover, Phys. Rev. **123** (1961) 267; **127** (1962) 2142;
J. R. Grover and J. Gilat, Phys. Rev. **157** (1967) 814
19) N. T. Porile, Low-energy nuclear reactions, Nuclear chemistry, ed. L. Yaffe (Academic Press, New York, 1968)
20) S. Liran and N. Zeldes, Nucl. Phys. **A136** (1969) 190
21) J. H. E. Mattauch, W. Thiele and A. H. Wapstra, Nucl. Phys. **67** (1965) 1, 73
22) J. Wing and J. Varley, ANL 6886 (1964) unpublished
23) W. D. Myers and W. J. Swiatecki, Nucl. Phys. **81** (1966) 1
24) A. G. W. Cameron, Can. J. Phys. **36** (1958) 1040;
A. G. W. Cameron and R. M. Elkin, Can. J. Phys. **43** (1965) 1288;
P. E. Nemirowski and Yu. V. Adamchuck, Nucl. Phys. **39** (1962) 551
25) D. Vinciguerra, K. Kotajima and R. E. van de Vijver, Nucl. Phys. **77** (1966) 337
26) A. Lindner, IKF-17, EANDC (E) 73 "U", unpublished
27) F. G. Perey and B. Buck, Nucl. Phys. **32** (1962) 353
28) J. M. B. Lang and K. J. Le Couteur, Proc. Phys. Soc. **A67** (1964) 585
29) E. Erba, U. Facchini and E. Saetta Menichella, Nuovo Cim. **22** (1962) 1237
30) E. Gadioli, I. Iori, N. Molho and L. Zetta, Nucl. Phys. **A138** (1969) 321
31) Y. Le Beyec and M. Lefort, Nucl. Phys. **A99** (1967) 131
32) V. M. Strutinsky, Nucl. Phys. **A95** (1967) 420
33) V. M. Strutinsky and H. C. Pauli, Report in physics and chemistry of fission (IAEA, Vienna, 1969)